Supporting Information

High Proton Conductivity in $Ba_5Er_2Al_2ZrO_{13}$, a Hexagonal Perovskite-Related Oxide with Intrinsically Oxygen-Deficient Layers

Taito Murakami,[1] James R. Hester,[2] and Masatomo Yashima[1]*

[1] *Department of Chemistry, School of Science, Tokyo Institute of Technology, 2-12-1-W4-17, O-okayama, Meguro-ku, Tokyo, 152-8551*

[2] *Australian Centre for Neutron Scattering, Australian Nuclear Science and Technology Organisation (ANSTO), Locked Bag 2001, Kirrawee DC, NSW, 2232, Australia*

* Corresponding author: yashima@cms.titech.ac.jp

Experimental Procedure

Polycrystalline samples of $Ba_5M_2Al_2ZrO_{13}$ (M = Dy, Er, Tm, Yb, Lu) were synthesized via high-temperature solid-state reactions using the starting materials of $BaCO_3$ (99.95%, Kojund Chemical), Dy_2O_3 (99.9%, Shin-Etsu Chemical), Er_2O_3 (99.9%, Shin-Etsu Chemical), Tm_2O_3 (99.9%, Shin-Etsu Chemical), Yb_2O_3 (99.9%, Shin-Etsu Chemical), Lu_2O_3 (99.9%, Shin-Etsu Chemical), Al_2O_3 (99.99%, Kojund Chemical), and ZrO_2 (99.9%, Soekawa Chemical). Stoichiometric amounts of the starting materials were mixed and ground in an agate mortar, followed by heating at 900 °C for 10 hours in air. The calcined mixture was crushed, ground, pelletized at about 100 MPa, and heated at 1600 °C for 10 hours in air. The obtained pellet was crushed in a WC mortar and used for further investigations.

The phase purity of $Ba_5M_2Al_2ZrO_{13}$ (M = Dy, Er, Tm, Yb, Lu) was examined by the X-ray powder diffraction experiments with Bruker AXS D8 Advance using Cu $K\alpha$ radiation. The chemical composition of $Ba_5Er_2Al_2ZrO_{13}$ powders was examined by inductively coupled plasma atomic emission spectroscopy (ICP-AES). X-ray photoelectron spectroscopy (XPS) spectra of $Ba_5Er_2Al_2ZrO_{13}$ were measured by an X-ray photoelectron spectrometer. Thermogravimetric (TG) data of $Ba_5Er_2Al_2ZrO_{13}$ were collected in wet (water vapor partial pressure $P(H_2O)$ = 0.017 atm) and dry air ($P(H_2O) < 10^{-5}$ atm) with heating and cooling rates of 5 °C min^{-1}. The neutron-diffraction measurements of $Ba_5Er_2Al_2ZrO_{13}$ were carried out using a fixed-wavelength neutron diffractometer ECHIDNA with λ = 1.622543(12) Å at Australian Nuclear Science and Technology Organization (ANSTO). The collected data were analyzed by the Rietveld method with Jana2006 program.[1]

The electrical conductivities of $Ba_5M_2Al_2ZrO_{13}$ (M = Dy, Er, Tm, Yb, Lu) were measured using a DC 4-probe method using sintered pellets with Pt electrodes at temperatures ranging from 300 °C to 1200 °C. The typical relative density of pellets sintered at 1600 °C are 65~70%. Pt-paste electrodes with Pt wires were attached to the sintered products and heated at 1000 °C for 1 hour to remove organics in the Pt paste. The total and proton conductivity of fully dense material σ_{tot} and σ_H were estimated from the measured conductivities (σ_{tot}^{mea} and σ_H^{mea}) and relative density d according to the following equations.[2]

$$\sigma_{tot} = \sigma_{tot}^{mea} \frac{2}{2-3p}$$

$$\sigma_H = \sigma_H^{mea} \frac{2}{2-3p}$$

where p is the pore volume fraction and $p = 1-d$. The oxygen partial pressure $P(O_2)$ dependencies of the electrical conductivity for $Ba_5Er_2Al_2ZrO_{13}$ were measured at 400, 600, and 800 °C using O_2, N_2 and N_2/H_2 gas mixtures in both dry and wet conditions. The $P(O_2)$ was monitored by an oxygen sensor. Wet air was obtained by passing the gas through a glass tube containing distilled water at 15 °C. Bond-valence-based energy landscape for a test proton in $Ba_5Er_2Al_2ZrO_{13}$ was investigated by the bond valence (BV) method using softBV program.[3] The crystal structures and BV-based energy landscapes were drawn with VESTA.[4]

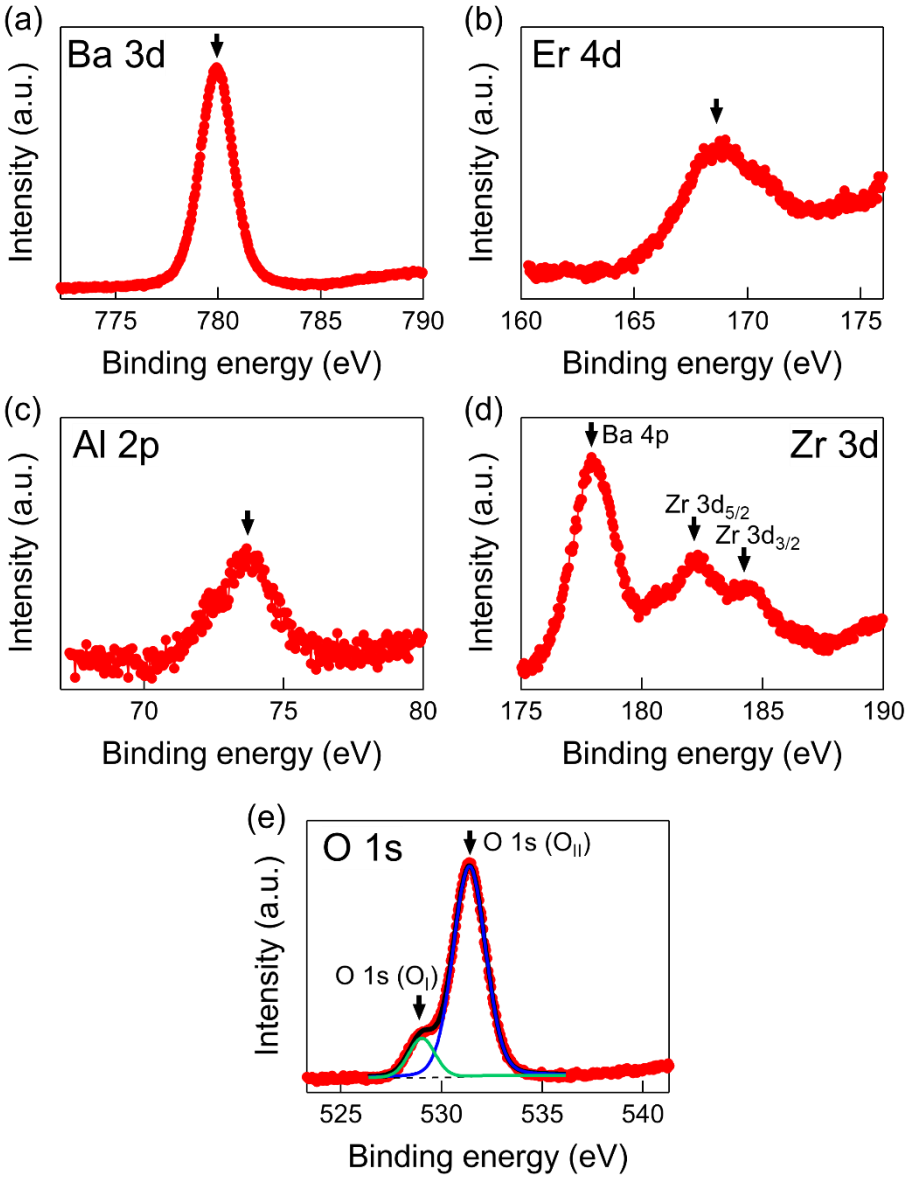

Figure S1. XPS spectra of (a) Ba 3d, (b) Er 4d, (c) Al 2p, (d) Zr 3d, and (e) O 1s in $Ba_5Er_2Al_2ZrO_{13.23}H_{0.46}$.

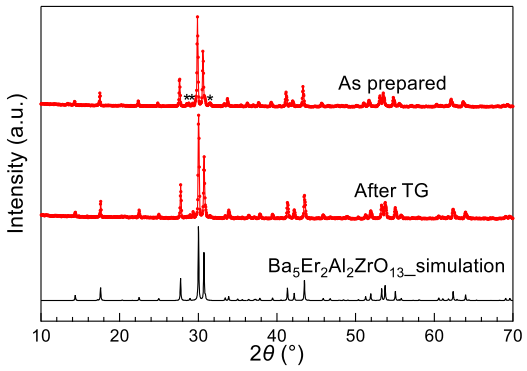

Figure S2. Cu *Kα* X-ray powder diffraction patterns of $Ba_5Er_2Al_2ZrO_{13.23}\cdot xH_2O$ before and after the TG analyses along with the simulation pattern. Several unindexed peaks (not assigned as any superreflections) are denoted by asterisk symbols. The simulation data were taken from the reference.[5]

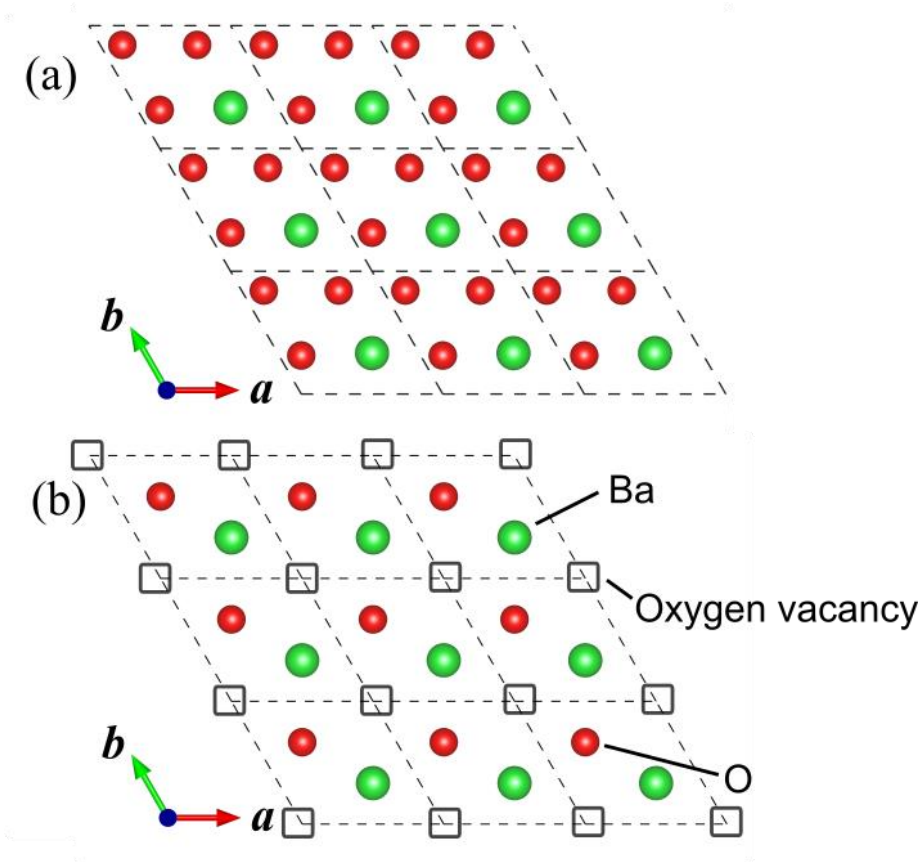

Figure S3. (a) Close packed BaO_3 and (b) inherently oxygen deficient BaO (h′) layers viewed along the *c* axis. Green and red spheres represent Ba and O ions, respectively. The open squares denote the oxygen vacancies, which forms the inherently oxygen deficient layer.

Thermogravimetric analyses for $Ba_5Er_2Al_2ZrO_{13}$

Thermogravimetric (TG) analyses of as-prepared $Ba_5Er_2Al_2ZrO_{13}$ were carried out on heating and cooling in wet and dry air. To examine the reversibility, reproducibility and the effect of surface contamination, we measured the TG data continuously three times using the same sample.

On the 1st heating in wet air ($P(H_2O)$ = 0.017 atm), a weight loss of 1.5 wt% was observed (Figure S4a), which indicates a release of H_2O, O_2 and/or CO_2. In wet air, the weight gain of approximately 0.8 wt% was observed on the 1st, 2nd and 3rd cooling and weight loss of approximately 0.8 wt% is seen on the 2nd and 3rd heating, which indicates the reproducibility. The larger weight loss on the 1st heating is mainly attributable to the release of H_2O on the sample surface.

On the 1st heating in dry air ($P(H_2O) < 10^{-5}$ atm), a weight loss of 0.7 wt% was observed (Figure S4b), which indicates a release of H_2O, O_2 and/or CO_2. In dry air, the weight gains of approximately 0.4 wt% were observed on the 1st, 2nd and 3rd cooling, which shows the reproducibility. Weight losses of approximately 0.4 wt% are seen on the 2nd and 3rd heating, which indicates the reversibility and reproducibility. The larger weight loss on the 1st heating is mainly attributable to the release of H_2O on the sample surface.

The weight losses on 2nd and 3rd heating in wet air (0.8 wt%) are larger than those in dry air (0.4 wt%), indicating that the released gas in wet air includes H_2O. Considering the difference of weight change between the wet and dry air, at least ≈0.2 H_2O in $Ba_5Er_2Al_2ZrO_{13}$ is deduced. The weight losses on the 2nd and 3rd heating in dry air are mainly attributable to O2 gas release. After the TG measurements, no sample decomposition was observed, demonstrating the high phase stability of $Ba_5Er_2Al_2ZrO_{13}$ up to 1200 °C (see the XRD patterns in Figure S2).

The actual loading of water in the sample has been evaluated as follows. The sample was heated at 1200 °C for 2 hours in dry air ($P(H_2O) < 10^{-5}$ atm) to remove absorbed H_2O and CO_2. Subsequently, the gas was switched to wet air ($P(H_2O)$≈0.021 atm), and the weight of the sample saturated with water was measured on cooling in equilibrium isotherms. TG data were collected from 1000 °C to room temperature (every 100 °C), with 3 h stabilization time at each temperature (Figure S5). The procedure was repeated in dry air, which was used as reference state. The actual water amount was estimated from the difference between the TG measurements performed in dry and wet air. The loaded water amount at room temperature corresponds to ≈0.27 H_2O per formula unit.

Using the amount of water uptake obtained from the TG measurements, we could derive the equilibrium constant for the water incorporation reaction using the Kröger-Vink notation. The crystal structure of $Ba_5Er_2Al_2ZrO_{13}$ has inherently oxygen-deficient (h′) layers, where the water uptake may take place. Here, the reaction of water incorporation can be expressed as

$$H_2O(g) + 2O_{O3}^{\times} + V_{O4}^{\times} \leftrightarrow 2(O_{O3}H)^{\bullet} + O_{O4}''$$

where protons are assumed to be exclusively bonded to the oxygen atom at the O3 site, as supported by Rietveld analysis of neutron-diffraction data (Fig. S8).

The equilibrium constant is

$$K_W = \frac{[(O_{O3}H)^{\bullet}]^2[O_{O4}'']}{P(H_2O)\,[O_{O3}^{\times}]^2[V_{O4}^{\times}]}$$

The electroneutrality condition is

$$[(O_{O3}H)^{\bullet}] = 2[O_{O4}'']$$

The conservations of the total numbers of oxygen atoms and vacancies at the O4 and O3 sites are expressed as,

$$[V_{O4}^{\times}] + [O_{O4}''] = 1$$
$$[O_{O3}^{\times}] + [(O_{O3}H)^{\bullet}] = 1$$

As a result, the equilibrium constant for the water incorporation reaction can be written as a function of OH^- concentration:

$$K_W = \frac{\frac{1}{2}[(O_{O3}H)^{\bullet}]^3}{P(H_2O)\,(1-[(O_{O3}H)^{\bullet}])^2(1-\frac{1}{2}[(O_{O3}H)^{\bullet}])}$$

From the relation of $K_W = \exp[(-\Delta H^0 + T\Delta S^0)/RT]$, we can estimate the enthalpy (ΔH^0) and entropy (ΔS^0) of the water incorporation reaction.

The temperature dependence of equilibrium constant (Figure S7) shows non-Arrhenius behaviour, where two different hydration regimes, inferring two-step hydration process below and above 400 °C. The reaction enthalpy and entropy below 400 °C are calculated to be ΔH^0 = -13(6) kJ mol^{-1} and ΔS^0 = 21(16) kJ K^{-1}mol^{-1}, respectively. At temperatures higher than 400 °C, the values are ΔH^0 = -192(15) kJ mol^{-1} and ΔS^0 = -257(18) kJ K^{-1} mol^{-1}, comparable to those obtained for other proton conductors.[6]

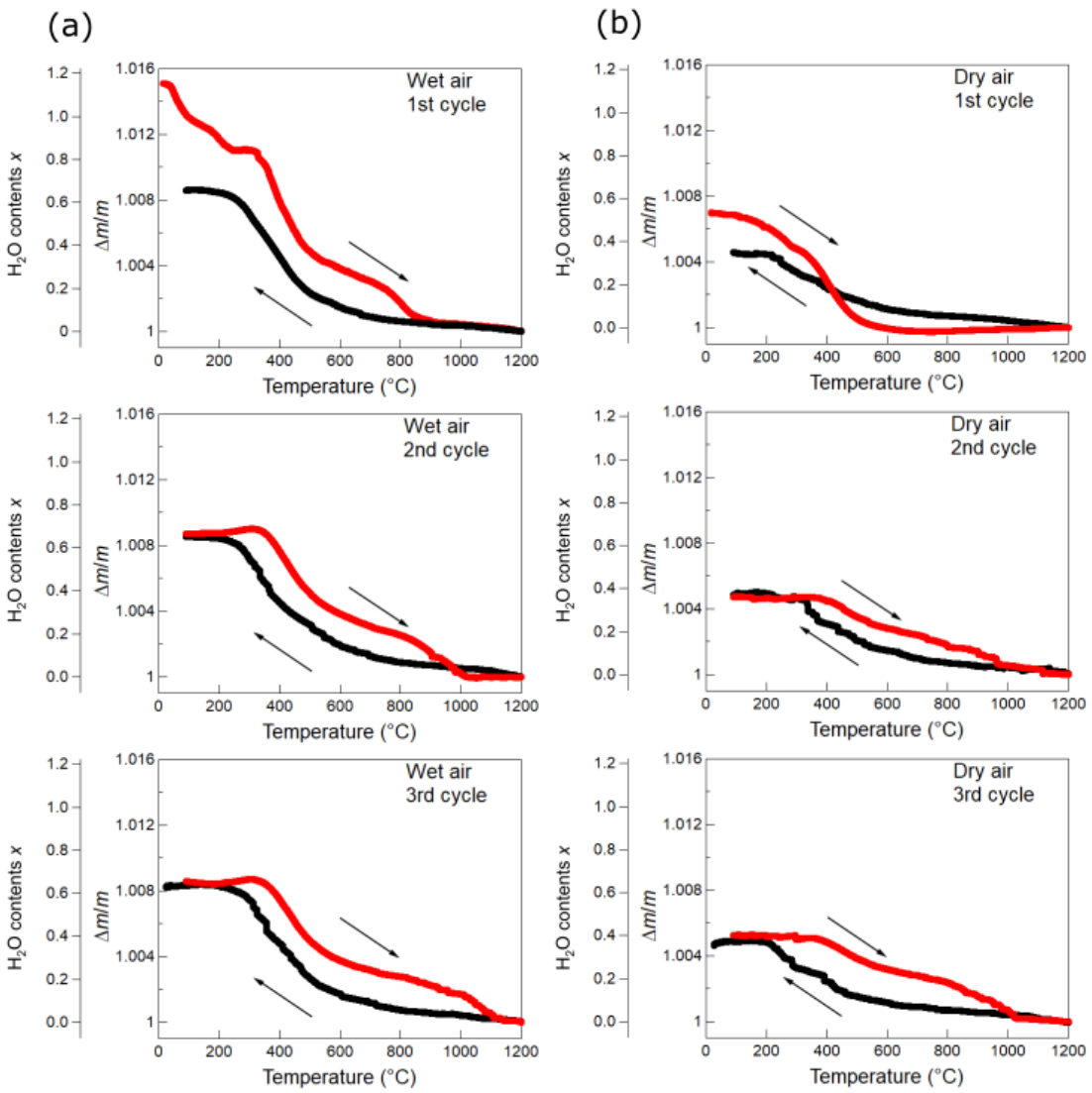

Figure S4. TG data of as-prepared $Ba_5Er_2Al_2ZrO_{13}{\cdot}xH_2O$ collected in (a) wet ($P(H_2O)$ = 0.017 atm) and (b) dry ($P(H_2O) < 10^{-5}$ atm) air. The H_2O contents x in $Ba_5Er_2Al_2ZrO_{13}{\cdot}xH_2O$ on heating and cooling are plotted, postulating that the sample contains no H_2O ($x = 0$) at 1200 °C and are oxygen-stoichiometric composition of $Ba_5Er_2Al_2ZrO_{13}$. In the first cycle, on heating, the weight loss is larger than those in the second and third cycles, which is attributable to surface H_2O, O_2 and/or CO_2. $\Delta m/m$ represents the ratio of the weight change ($m - m_0$) relative to weight at 1200 °C, m_0:

$$\Delta m/m = (m - m_0)/m_0.$$

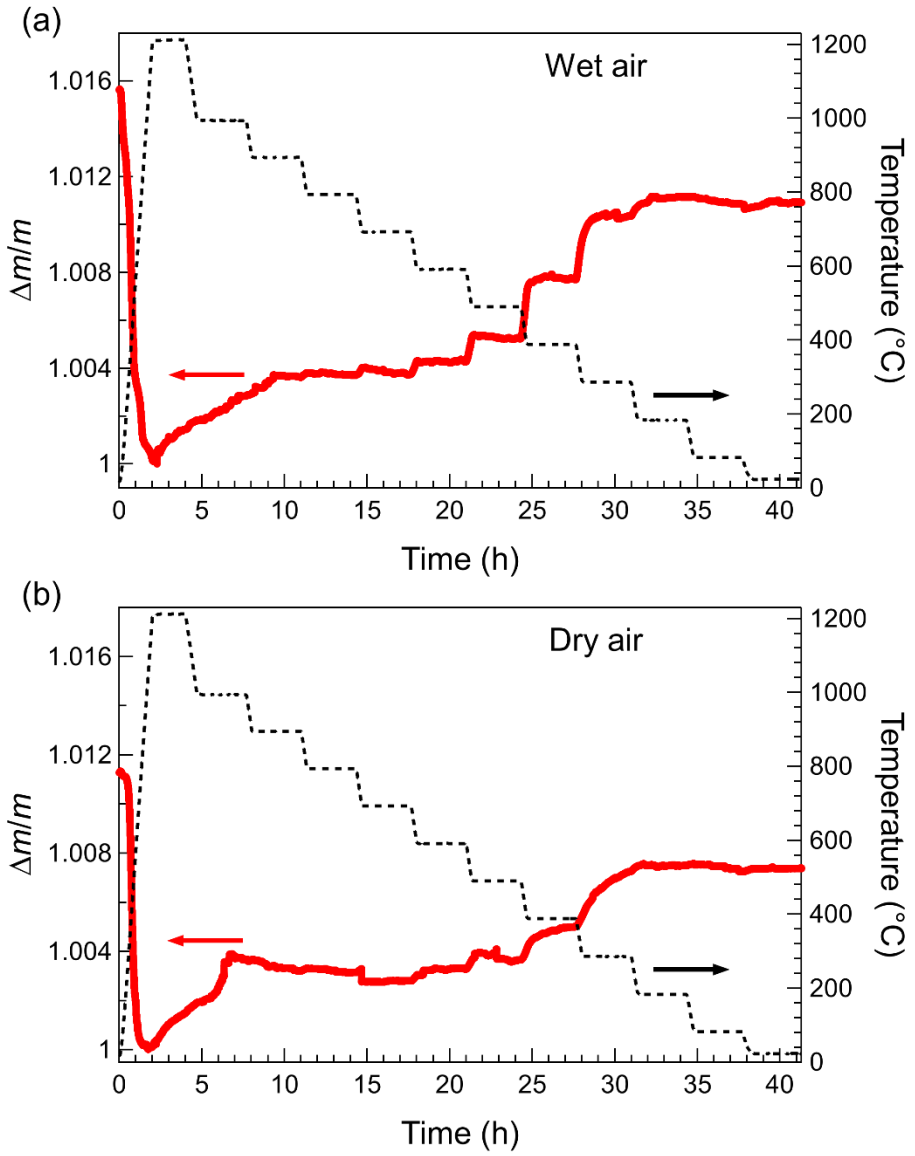

Figure S5. Weight change of $Ba_5Er_2Al_2ZrO_{13}{\cdot}xH_2O$ and temperature as a function of time in (a) wet ($P(H_2O) = 0.021$ atm) and (b) dry ($P(H_2O) < 10^{-5}$ atm) air. $\Delta m/m$ represents the ratio of the weight change ($m - m_0$) relative to weight at 1200 °C, m_0: $\Delta m/m = (m - m_0)/m_0$.

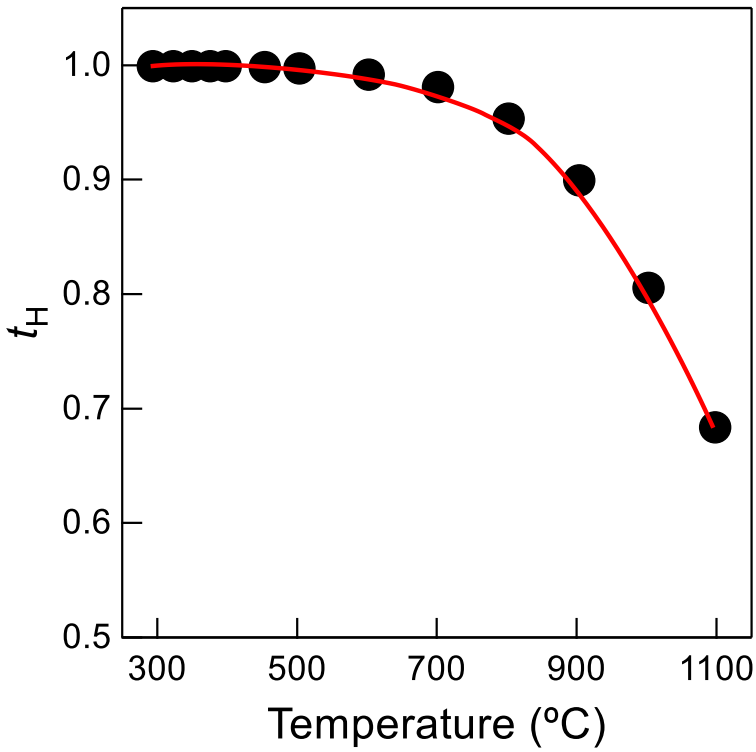

Figure S6. Temperature dependence of the calculated proton transport number (t_H) of $Ba_5Er_2Al_2ZrO_{13.23}$ $\cdot xH_2O$ according to the following relation: $t_H = \sigma_H / \sigma_{wet} = (\sigma_{wet} - \sigma_{dry}) / \sigma_{wet}$, where σ_{wet} and σ_{dry} represent the total electrical conductivities in wet ($P(H_2O)$ = 0.017 atm) and dry ($P(H_2O) < 10^{-5}$ atm) air, respectively.

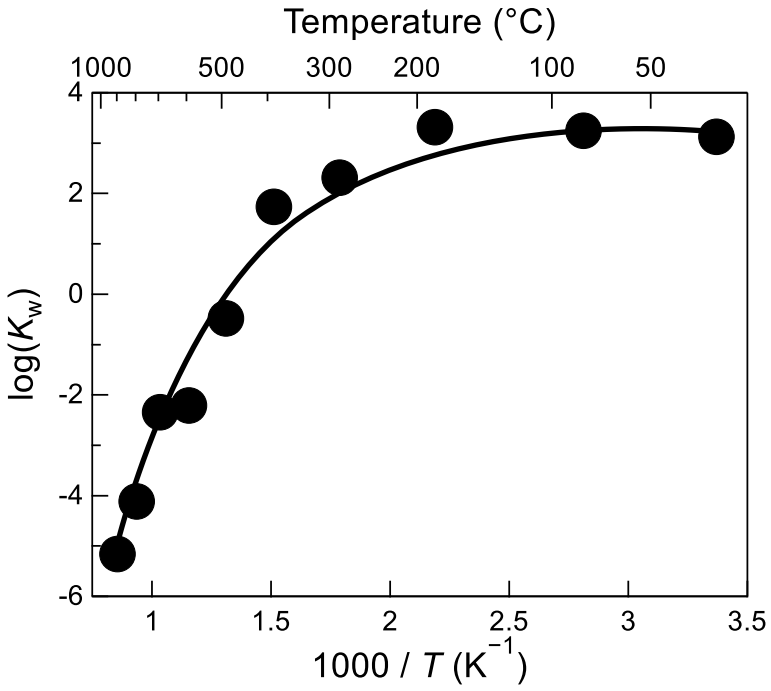

Figure S7. Temperature dependence of the equilibrium constant K_w for the water incorporation reaction of $Ba_5Er_2Al_2ZrO_{13.23}{\cdot}xH_2O$.

Table S1. Refined crystal parameters and reliability factors in Rietveld analysis of the neutron diffraction data for $Ba_5Er_2Al_2ZrO_{13}$ without considering protons.[a, b]

Site label	Wyckoff position	x	Y	z	U_{eq} (Å^2)[c]	g[d]	BVS[e]
Ba1	4*e*	0	0	0.3591(3)	0.0353(8)	1	1.916
Ba2	4*f*	2/3	1/3	0.5446(3)	0.0353(8)	1	1.668
Ba3	2*d*	2/3	1/3	1/4	0.0353(8)	1	1.401
Zr	2*a*	0	0	0	0.0344(18)	1	3.940
Er	4*f*	2/3	1/3	0.39617(15)	0.0235(7)	1	3.163
Al	4*f*	2/3	1/3	0.8174(3)	0.0177(11)[g]	1	3.281
O1	12*k*	0.5079(5)	0.0158(9)	0.65796(15)	0.0620(16)	1	1.821
O2	12*k*	0.3256(8)	0.1628(4)	0.45000(12)	0.0401(9)	1	1.936
O3	6*h*	0.2981(17)	0.596(3)	1/4	0.065(9)	1/3	2.063
O4	2*b*	0	0	1/4	0.089(17)[g]	0.31(4)	
Site label	U_{11} (Å^2)	U_{22} (Å^2)	U_{33} (Å^2)	U_{12} (Å^2)	U_{13} (Å^2)	U_{23} (Å^2)	
Ba1	0.0360(9)	0.0360(9)	0.034(2)	0.0180(4)	0	0	
Ba2	0.0360(9)[f]	0.0360(9)[f]	0.034(2)[f]	0.0180(4)[f]	0	0	
Ba3	0.0360(9)[f]	0.0360(9)[f]	0.034(2)[f]	0.0180(4)[f]	0	0	
Zr	0.0341(19)	0.0341(19)	0.035(4)	0.0171(9)	0	0	
Er	0.0231(8)	0.0231(8)	0.0242(16)	0.0115(4)	0	0	
O1	0.0562(17)	0.037(2)	0.086(3)	0.0184(10)	−0.0176(11)	−0.035(2)	
O2	0.0274(13)	0.0399(10)	0.0490(15)	0.0137(6)	0.0133(12)	0.0066(6)	
O3	0.104(14)	0.055(13)	0.019(5)	0.027(6)	0	0	

[a] Values in parentheses for refined parameters indicate the estimated standard deviations.

[b] Space group: $P6_3/mmc$, $Z = 2$, $a = 5.95788(8)$ Å, $c = 24.6923(6)$ Å, $R_{wp} = 2.80\%$, $R_p = 2.18\%$, $R_B = 5.83\%$, and $R_F = 3.69\%$.

[c] Equivalent isotropic atomic displacement parameter.

[d] The occupancy of *X* atom at the *Xn* site. Occupancies are fixed to 1 at Ba1, Ba2, Ba3, Zr, Er, Al, O1, and O2 site, fixed to 1/3 at O3 site, and allowed to vary at O4 site.

[e] Bond valence sum. Each bond valence parameter was taken from the literature.[7,8]

[f] Linear constraints: U_{11}(Ba1) = U_{11}(Ba2) = U_{11}(Ba3) and U_{33}(Ba1) = U_{33}(Ba2) = U_{33}(Ba3).

[g] U_{iso}: Refined isotropic atomic displacement parameter.

Table S2. Refined crystal parameters and reliability factors in Rietveld analysis of the neutron diffraction data for $Ba_5Er_2Al_2ZrO_{13.23}H_{0.46}$. [a, b]

Site label	Wyckoff position	x	y	z	U_{eq} (Å^2)[c]	g[d]	BVS[e]
Ba1	4*e*	0	0	0.3592(3)	0.0399(8)	1	1.914
Ba2	4*f*	2/3	1/3	0.5445(3)	0.0399(8)	1	1.669
Ba3	2*d*	2/3	1/3	1/4	0.0399(8)	1	1.421
Zr	2*a*	0	0	0	0.0388(17)	1	3.95
Er	4*f*	2/3	1/3	0.39616(15)	0.0286(7)	1	3.191
Al	4*f*	2/3	1/3	0.8174(3)	0.0242(11)[e]	1	3.223
O1	12*k*	0.5069(5)	0.0138(9)	0.65819(15)	0.0674(16)	1	1.816
O2	12*k*	0.3257(8)	0.1628(4)	0.45003(12)	0.0444(9)	1	1.941
O3	6*h*	0.301(3)	0.603(6)	1/4	0.094(13)	1/3	2.068
O4	2*b*	0	0	1/4	0.067(14)[g,h]	0.23(3)[h]	
H	6*h*	0.461(5)	0.921(10)	1/4	0.067(14)[g,h]	0.15(2)[h]	
Site label	U_{11} (Å^2)	U_{22} (Å^2)	U_{33} (Å^2)	U_{12} (Å^2)	U_{13} (Å^2)	U_{23} (Å^2)	
Ba1	0.0406(9)	0.0406(9)	0.038(2)	0.0203(4)	0	0	
Ba2	0.0406(9)[f]	0.0406(9)[f]	0.038(2)[f]	0.0203(4)[f]	0	0	
Ba3	0.0406(9)[f]	0.0406(9)[f]	0.038(2)[f]	0.0203(4)[f]	0	0	
Zr	0.0387(19)	0.0387(19)	0.039(4)	0.0193(9)	0	0	
Er	0.0278(7)	0.0278(7)	0.0303(17)	0.0139(4)	0	0	
O1	0.0613(17)	0.043(2)	0.092(3)	0.0216(10)	−0.0175(12)	−0.035(2)	
O2	0.0326(13)	0.0443(9)	0.0524(15)	0.0163(7)	0.0138(12)	0.0069(6)	
O3	0.16(2)	0.074(15)	0.018(5)	0.037(8)	0	0	

[a] Values in parentheses for refined parameters indicate one standard deviation.

[b] Space group: $P6_3/mmc$, $Z = 2$, $a = 5.95791(8)$ Å, $c = 24.6928(6)$ Å, $R_{wp} = 2.76\%$, $R_p = 2.18\%$, $R_B = 5.62\%$, and $R_F = 3.55\%$.

[c] Equivalent isotropic atomic displacement parameter.

[d] g represents the occupancy of X atom at the Xn site. Occupancies are fixed to 1 at Ba1, Ba2, Ba3, Zr, Er, Al, O1, and O2 site, fixed to 1/3 at O3 site, and allowed to vary at O4 and H sites.

[e] Bond valence sum. Each bond valence parameter was taken from the literature.[7,8]

[f] Linear constraints: U_{11}(Ba1) = U_{11}(Ba2) = U_{11}(Ba3) and U_{33}(Ba1) = U_{33}(Ba2) = U_{33}(Ba3).

[g] U_{iso}: Refined isotropic atomic displacement parameter.

[h] Linear constraints: U_{iso}(O4) = U_{iso}(H) and g(O4) = 3/2 g(H).

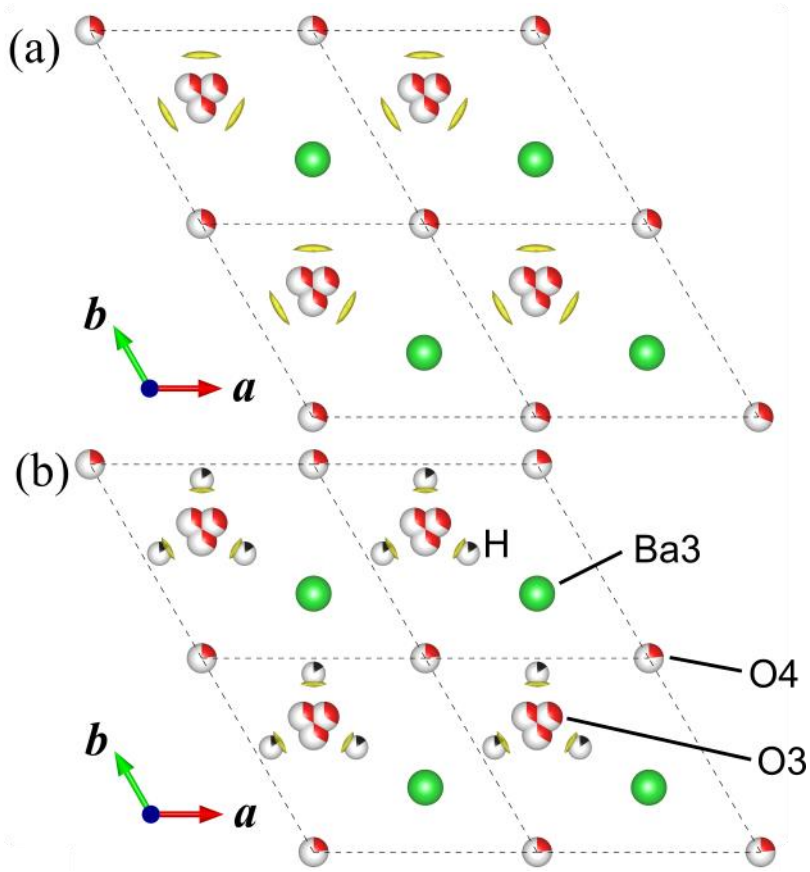

Figure S8. BV-based energy landscapes (BVELs) for a test proton for (a) $Ba_5Er_2Al_2ZrO_{13}$ and (b) $Ba_5Er_2Al_2ZrO_{13.23}H_{0.46}$ with the isosurface at 0.05 eV viewed along the *c* axis. Green, red/white, and black/white spheres represent Ba, O, and H, respectively. The split H and O3 sites are consistent with the BVELs for a proton and an oxide ion, respectively.

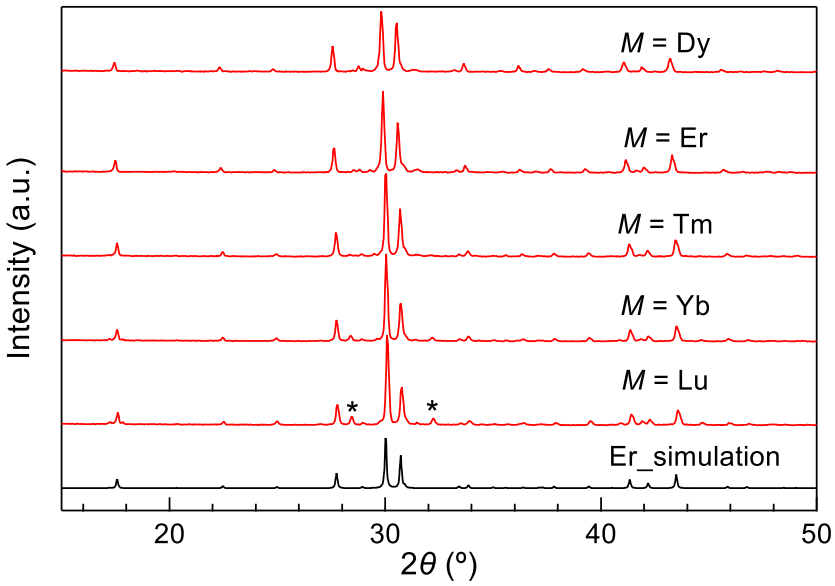

Figure S9. Cu *Kα* XRD patterns of $Ba_5M_2Al_2ZrO_{13}{\cdot}xH_2O$ (*M* = Dy, Er, Tm, Yb, and Lu). Several unindexed peaks (not assigned as any superreflections) are denoted by asterisk symbols. The simulation pattern was calculated using the crystal data in the literature.[5]

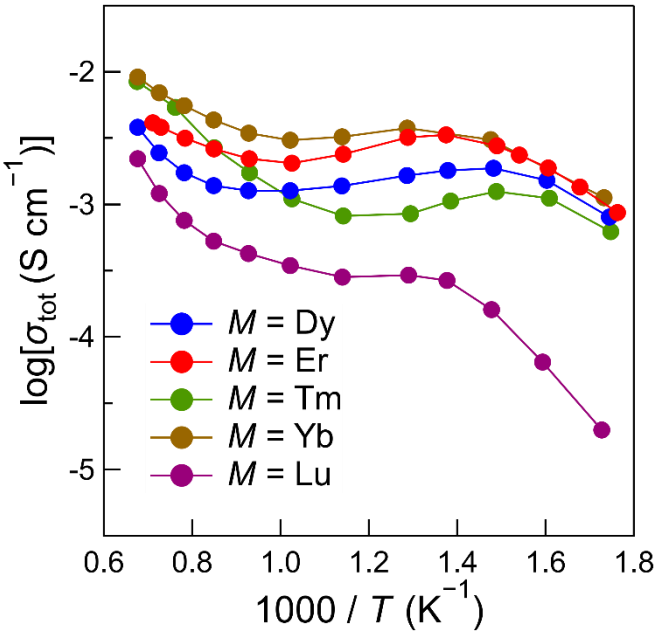

Figure S10. Arrhenius plots of the total electrical conductivity σ_{tot} of $Ba_5M_2Al_2ZrO_{13}\cdot xH_2O$ (M = Dy, Er, Tm, Yb, and Lu) in static air ($P(H_2O) \approx 0.02$ atm).

REFERENCES

(1) Petříček, V.; Dušek, M.; Palatinus, L. Crystallographic Computing System JANA2006: General Features. *Zeitschrift für Krist. Mater.* **2014**, *229* (5), 345–352.

(2) El Khal, H.; Cordier, A.; Batis, N.; Siebert, E.; Georges, S.; Steil, M. C. Effect of Porosity on the Electrical Conductivity of LAMOX Materials. *Solid State Ionics* **2017**, *304*, 75–84.

(3) Chen, H.; Wong, L. L.; Adams, S. SoftBV–a Software Tool for Screening the Materials Genome of Inorganic Fast Ion Conductors. *Acta Crystallogr. Sect. B Struct. Sci. Cryst. Eng. Mater.* **2019**, *75* (1), 18–33.

(4) Momma, K.; Izumi, F. VESTA 3 for Three-Dimensional Visualization of Crystal, Volumetric and Morphology Data. *J. Appl. Crystallogr.* **2011**, *44* (6), 1272–1276.

(5) Shpanchenko, R. V; Abakumov, A. M.; Antipov, E. V; Nistor, L.; Van Tendeloo, G.; Amelinckx, S. Structural Study of the New Complex Oxides $Ba_{5-y}Sr_yR_{2-x}Al_2Zr_{1+x}O_{13+x/2}$ (R= Gd–Lu, Y, Sc). *J. Solid State Chem.* **1995**, *118* (1), 180–192.

(6) Kreuer, K.-D. Proton-Conducting Oxides. *Annu. Rev. Mater. Res.* **2003**, *33* (1), 333–359.

(7) Brown, I. D.; Altermatt, D. Bond-Valence Parameters Obtained from a Systematic Analysis of the Inorganic Crystal Structure Database. *Acta Crystallogr. Sect. B Struct. Sci.* **1985**, *41* (4), 244–247.

(8) Brese, N. E.; O'keeffe, M. Bond-Valence Parameters for Solids. *Acta Crystallogr. Sect. B Struct. Sci.* **1991**, *47* (2), 192–197.